


A Facility for Research in Experimental Nuclear Astrophysics (FRENA) - A Proposal



A National Facility

Proposed by

Nuclear & Atomic Physics Group

Saha Institute of Nuclear Physics

Scheme

- **Introduction & Motivation**
- **Facilities proposed for research**
- **Scope of research**
- **Experimental limitations**

Nuclear Astrophysics involves study of

- Synthesis of Elements

- Evolution of Cosmic sites

(Early Universe, Interstellar medium, red giants, supernova)

Sophisticated Computer Models

These Models require nuclear data as input mainly on

- Reaction rates



Intense beams of different species in the keV-MeV range
to cover various stellar astrophysical conditions

**NO SINGLE ACCELERATOR IS GOOD ENOUGH TO COVER THE
ENTIRE ENERGY DOMAIN**

THERMONUCLEAR REACTIONS



QUIESCENT PROCESSES (hydrostatic equilibrium)

$T \sim 10^6 - 10^8 \text{ K}$

average interaction time

$\tau \sim \langle \sigma v \rangle^{-1} \sim 10^9 \text{ y}$

Unstable Nuclei do not
play significant role



Dedicated Low Energy, High
Current Stable beams



EXPLOSIVE BURNING

$T > 10^8 \text{ K}$

average interaction time

$\tau \sim \langle \sigma v \rangle^{-1} \sim \text{seconds}$

Unstable Nuclei govern

Nuclear reactions

(r-, rp-process)



Generally using RIB

- Thin targets of high purity and stability
- Detector system with high sensitivity and energy resolution
- Efficient background reduction

Existing Experimental Facilities (Worldwide)

Radioactive Ion Beam Facilities

- HRIBF at Oak Ridge National Laboratory
- TRIUMF, Canada
- RIB, RIKEN, Japan
- SPIRAL, France

Stable Beam Facility

- LUNA, Gran Sasso, Italy
- LENA, TUNL, USA
- ERNA, Bochum, Germany
- ORELA, USA
- Karlsruhe, Germany

Indian Scenario

Four major Accelerators Centres in India

- 15MV Nuclear Science Centre (New Delhi)
- BARC-TIFR 14MV Pelletron (Mumbai)
- Variable Energy Cyclotron (Kolkata)
- 3 MV Tandem Accelerator at IOP, Bhubaneswar

Difficulties in their use in the study of Nuclear Astrophysics

- Cannot be operated at low terminal voltages
- Maximum beam currents ~ few hundred nano amperes

FRENA (Stable Beam)

(Facility for Research in Low Energy Nuclear Astrophysics)

FRENA + RIB at NSC and upcoming RIB at VECC

➡ Explore a wide range of problems in Nuclear Astrophysics

FUTURE ➤ Underground Laboratory of INO Project may house a very Low energy Accelerator

FRENA is proposed to include

Phase I

- Low Energy, high current Accelerator;
- High efficiency detector systems
- Data acquisition systems
- Target laboratory

Phase II

- Additional beam-lines
- Augmentation of detector systems
- Magnetic spectrograph
- Neutron induced studies

The Accelerator

- Terminal Voltage - 0.2 to 3.0 MV
- Typical Beam Currents:
 - H⁺ - ~1 mA
 - He²⁺ - 200 μA
 - Heavier Ions - 20 - 50 μA
- Pulsed beam of H⁺, ²H⁺ and He²⁺ (Phase I)
- Beam Energy can be varied in steps of a few keV.
- Switching Magnet to provide beams to 5 ports.
- Terminal Voltage stability - ±300 V
- Terminal Voltage ripple - 30 Vpp
- 90° Analyzing Magnet before switching magnet

This will be a unique accelerator in India in terms of low Energy and high current.

Detection and Detector systems

At low energies the compound nucleus (CN) reaction is the dominant process. The CN decays to different channels forming different products. The method employed to determine reaction cross-sections depends on the type of products to be detected.

The methods can be broadly classified as:

- (i) Light particle method,
- (ii) Heavy residue method,
- (iii) Gamma ray method, and
- (iv) Residual activity method.

The available detector systems at SINP can be fruitfully utilized.

These include

- The *INGA facility*, consisting of high efficiency *Compton suppressed Clover detector*;
- Array of large NaI(Tl) scintillators with 4π coverage, can be used a Sum spectrometer to measure total γ -ray yield;
- ΔE -E telescope with optimized combinations of ionization chambers and Si detectors;
- Micro-channel plates

Development of new detector systems includes

- High granularity detectors, like segmented Ge-clover or Ge-cluster detectors with tracking capability,
- Large-area curved Si-strip detector arrays or Si-strip detector boxes for the detection of light reaction products.
- The Phase II of the Proposal includes a Recoil separator with a high beam rejection efficiency, for detection of recoil products in the inverse kinematics. Use of ΔE -E telescopes and TOF for unique identification of recoil products.

TOF and coincidence techniques with reaction recoil particles and recoil gamma to uniquely identify low cross section events and reject cosmic-ray and beam-induced background contributions.

The high current Isotope Separator Facility at Saha Institute of Nuclear Physics, Kolkata can be envisioned as a support facility to supply the necessary isotopes.

Reasons behind opting for the 3 MV Accelerator

- As beginners in the field of Nuclear Astrophysics, we have decided not to go for a dedicated accelerator that is more suited for studying a very few specific reactions. Instead, we want to have a facility which can be used to study a wider range of problems in Nuclear Astrophysics.
- The relatively higher energy beams ($E_{\max}=1$ MeV/amu for ^{12}C) can be used fruitfully for studying heavy-ion fusion reactions, in particular, that dominate the late burning phases inside stars.
- Large energy span will permit a particular reaction to be studied over a wide energy region.

Study of Nuclear Astrophysics with the Proposed Facility

STELLAR NUCLEOSYNTHESIS

Thermonuclear Reactions at the Core of the Star

Non-Resonant Process

- One-step process
- Occurs at all energies
- Weak Energy dependence

Resonant Process

- Two-step process
- Occurs at specific energies
- Strong energy dependence

Non-Resonant Process

Reaction rate per particle-pair $\langle \sigma v \rangle$

where v – relative velocity of reaction partners;

$\varphi(v)$ - Maxwell-Boltzmann distribution for each of the reacting partners;

$$\langle \sigma v \rangle = \int_0^{\infty} \varphi(v) \cdot v \cdot \sigma(v) dv$$

$$\varphi_i(v) = 4\pi v^2 \left(\frac{\mu}{2\pi k_B T} \right)^{\frac{3}{2}} \exp \left(\frac{-\mu v^2}{2k_B T} \right)$$

$\sigma(v)$ – cross-section for the reaction
or

$\sigma(E_{cm})$ is expressed as a product of the penetrability through the Coulomb barrier and the so-called Astrophysical S-factor

$$\sigma(E_{CM}) = \frac{1}{E_{CM}} \cdot \exp(-2\pi\eta) \cdot S(E_{CM})$$

$$\eta \equiv zZ \cdot \alpha \cdot \sqrt{\frac{\mu c^2}{2E_{CM}}}$$

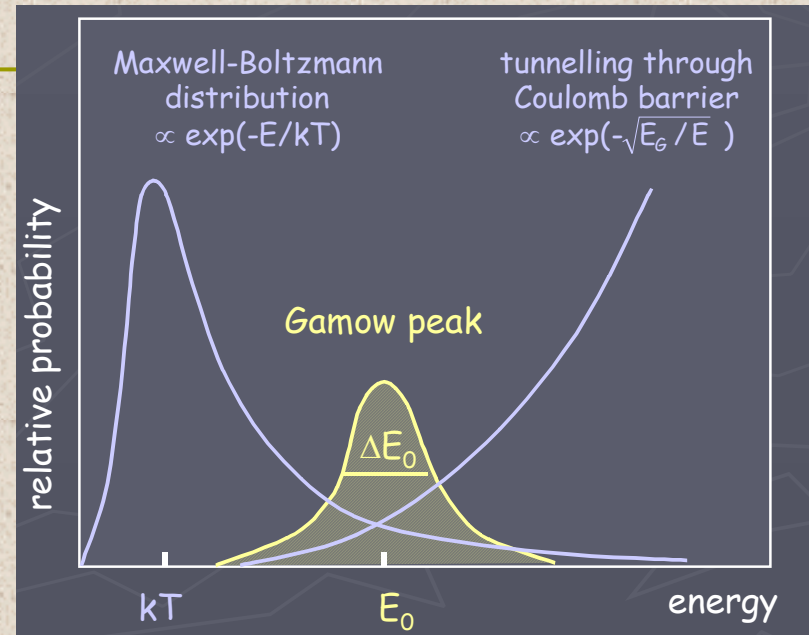
Reaction rate per particle-pair \longrightarrow

$$\langle \sigma v \rangle = \sqrt{\frac{8}{\pi\mu}} (k_B T)^{-\frac{3}{2}} \int_0^{\infty} S(E_{CM}) \cdot \exp \left(-\frac{E}{k_B T} - \frac{b}{\sqrt{E}} \right) dE_{CM}$$

Non-Resonant Process

Gamow Peak :
Most probable Energy
Region for
Thermonuclear Reaction

$$E_0 \pm \Delta E_0 / 2$$



**Astrophysical
S(E)-Factor**

$$\sigma(E) = \frac{1}{E} \exp(-2\pi\eta) S(E)$$

(for s-waves only!)

non-nuclear origin
STRONG energy
dependence

nuclear origin
WEAK energy
dependence

Examples: $T \sim 15 \times 10^6 \text{ K}$ ($T_6 = 15$)

reaction	Coulomb barrier (MeV)	E_0 (keV)	$\exp(-3E_0/kT) \Delta E_0$
$p + p$	0.55	5.9	7.0×10^{-6}
$\alpha + {}^{12}\text{C}$	3.43	56	5.9×10^{-56}
${}^{16}\text{O} + {}^{16}\text{O}$	14.07	237	2.5×10^{-237}

→ area of Gamow peak
(height \times width) $\sim \langle \sigma v \rangle$

STRONG sensitivity
to Coulomb barrier

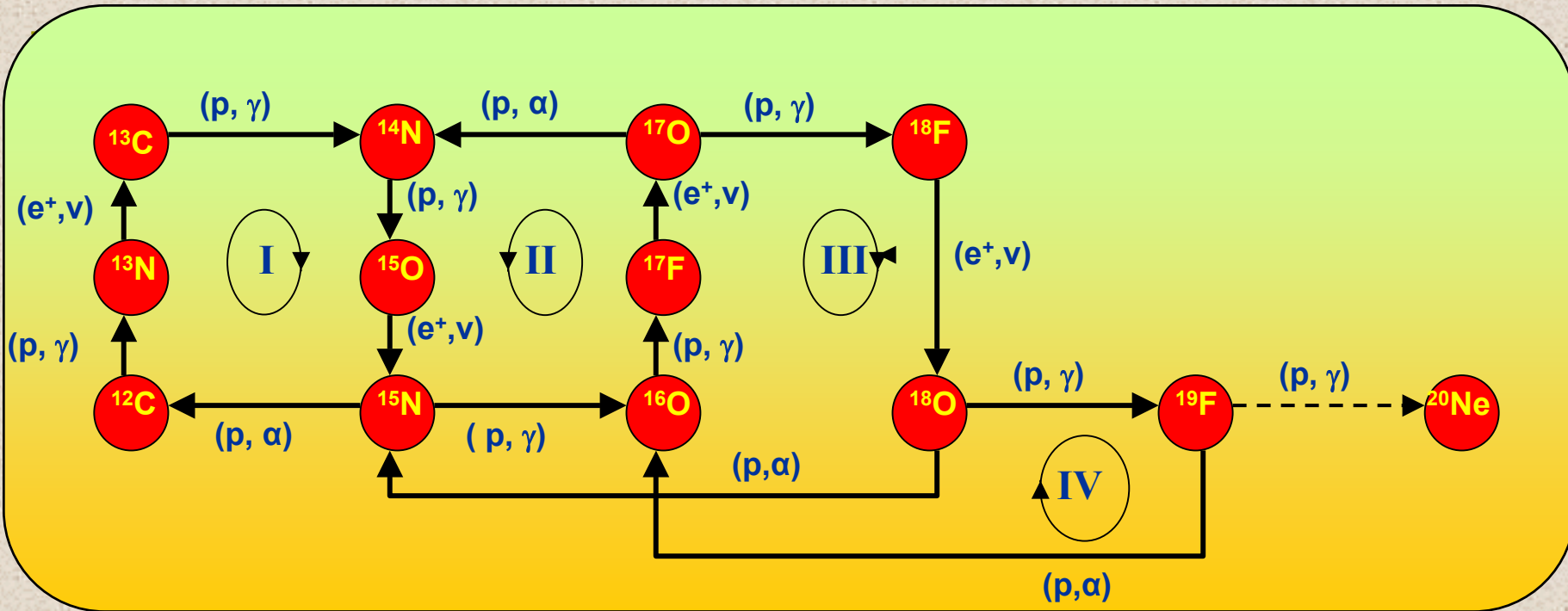
separate stages: H-burning
He-burning
C/O-burning ...

- Initially, only those nuclei with the smallest Coulomb barrier will react.
- Heavier elements will require correspondingly higher temperatures and are synthesized in well-defined phases, subsequently.
- H-, He-, C-, Ne-, O-, and Si-burning.

Some specific Reactions that can be studied

Reaction	Typical Temperature Range (X10 ⁹ K)	Gamow Peak E ₀ (MeV)	Gamow Window ΔE ₀ (MeV)	Energy avail. (MeV)
¹² C+ ¹² C	0.8–1.2	2.08–2.73	0.88–1.23	0.8-12
¹⁶ O+ ¹⁶ O	1.0–2.4	3.90-7.0	1.62–3.35	0.8-12
α+ ¹² C	0.2–0.6	0.31–0.66	0.17–0.42	0.6-9
α+ ¹⁶ O	0.2-3	0.39–1.77	0.19–1.56	0.6-9
p+ ¹⁴ N	0.2–3 0.16x10 ⁸ (Sun)	0.15–0.91 0.0274	0.12–1.12 0.007	0.4-6

CNO cycles



The reaction $^{14}\text{N}(p, \gamma)^{15}\text{O}$ is the slowest reaction in the CNO Cycles

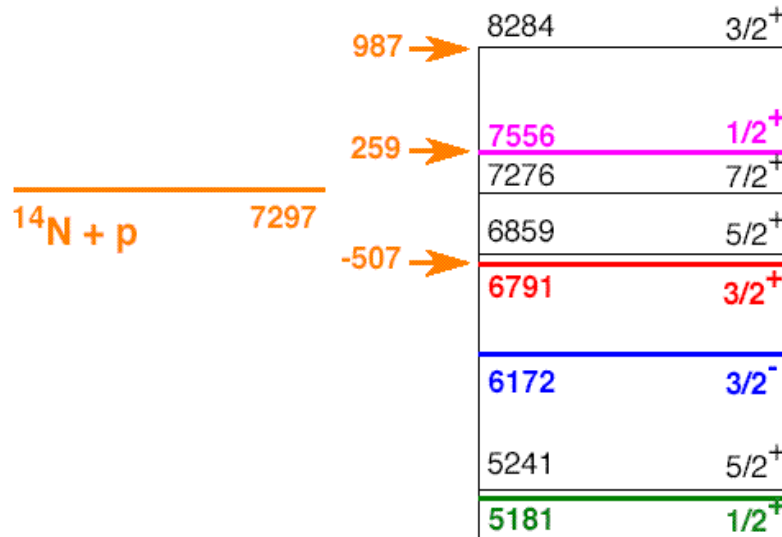
For
 $\rho = 100 \text{ g/cm}^3$,
 $X_{\text{H}} = 0.5$,
 $T_6 = 10$

Lifetimes (y)

$^{12}\text{C}(p, \gamma)^{13}\text{N} \text{ -- } 6.1 \times 10^9$
 $^{13}\text{C}(p, \gamma)^{14}\text{N} \text{ -- } 1.1 \times 10^9$
 $^{14}\text{N}(p, \gamma)^{15}\text{O} \text{ -- } 2.1 \times 10^{12}$
 $^{15}\text{N}(p, \alpha)^{12}\text{C} \text{ -- } 1.0 \times 10^8$

The reaction $^{14}\text{N}(p,\gamma)^{15}\text{O}$

Both direct capture and resonance reactions contribute to the reaction rate; sub-threshold states are important.



Recently, the $^{14}\text{N}(^3\text{He},d)^{15}\text{O}$ transfer reactions studied to deduce ANC's for $^{14}\text{N}(p,\gamma)^{15}\text{O}$

Reference	D/RC $\rightarrow 0$	D/RC $\rightarrow 6172$	D/RC $\rightarrow 6791$	Total
[Hebbard63]	0.27	1.00	1.40	2.67
[Schroeder87a]	1.55 ± 0.34	0.14 ± 0.05	1.41 ± 0.02	3.20 ± 0.54
[Angulo01]	$0.08^{+0.13}_{-0.06}$	$0.06^{+0.01}_{-0.02}$	1.63 ± 0.17	1.77 ± 0.20
[Bertone01]	0.12...0.45	see [Angulo01]	see [Angulo01]	≈ 2
[Mukh03]	0.15 ± 0.07	0.13 ± 0.02	1.40 ± 0.20	1.70 ± 0.22
[Formicola04a]	0.25 ± 0.06	see [Angulo01]	1.35 ± 0.05	$1.7^{+0.1(\text{stat})}_{\pm 0.2(\text{syst})}$

$S(0)$ values from different authors, in units of keV barn. Given is the sum of direct and resonant capture components (D/RC) into the states at 6791 and 6172 keV as well as the ground state of ^{15}O .

$$1804 \quad ^{14}\text{N} + ^3\text{He} - ^2\text{H}$$

$$^{15}\text{O} \quad J^\pi = 1/2^- \quad T = 1/2$$

The reaction $^{14}\text{N}(p,\gamma)^{15}\text{O}$ (*contd.*)

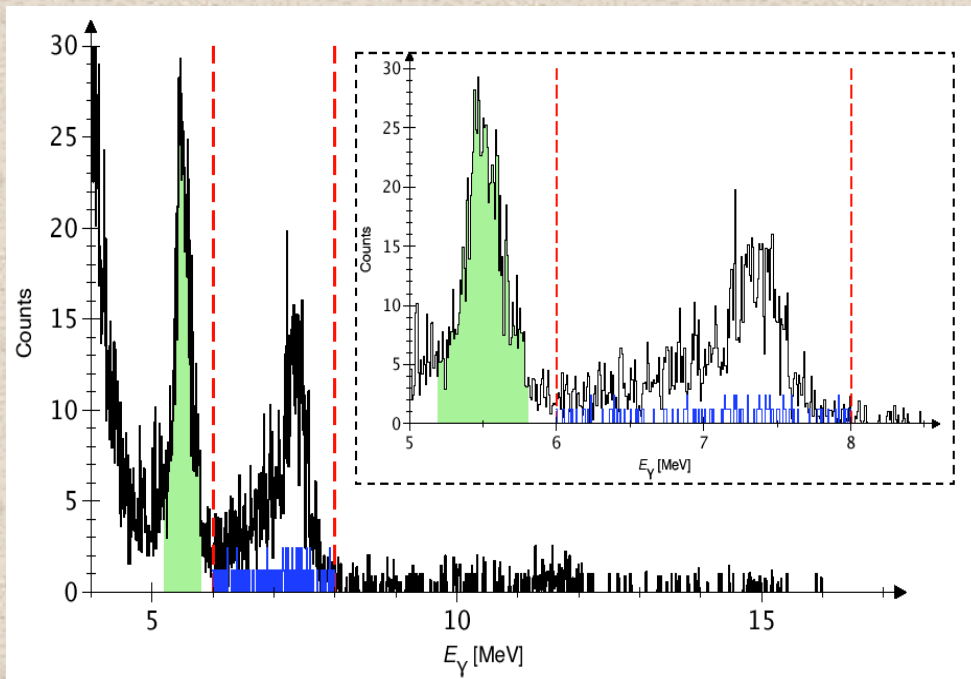
- Schröder al. concluded that $S(0)$ was dominated by two components:
 - (i) D/R capture into the 6791 keV state;
 - (ii) Resonant capture through the tail of 6791 keV state to the ground state.
- Using a $\Gamma_\gamma = 6.3$ eV for the 6791 keV state, $S(0) = 3.2 \pm 0.54$ keV barn.
- Recently, Bertone et al. measured the lifetime of the 6791 keV state to be $\tau = 1.60^{+0.75}_{-0.72}$ fs which corresponds to $\Gamma_\gamma = 0.41^{+0.34}_{-0.13}$ eV
- Reduced contribution from resonant capture to the ground state via the 6791 keV state
⇒ $S(0) = 1.77 \pm 0.20$ keV barn.

A very recent measurement

(carried out at LUNA2 400 kV Accelerator in the Gran Sasso under-Ground Laboratory, shielded by 3800 m (water equivalent) of rock)

Studied $^{14}\text{N}(p,\gamma)^{15}\text{O}$ at $E_{\text{cm}} = 90\text{-}230$ keV; gas target; lowest $\sigma = 3$ pbarn;
Detector – 4π BGO

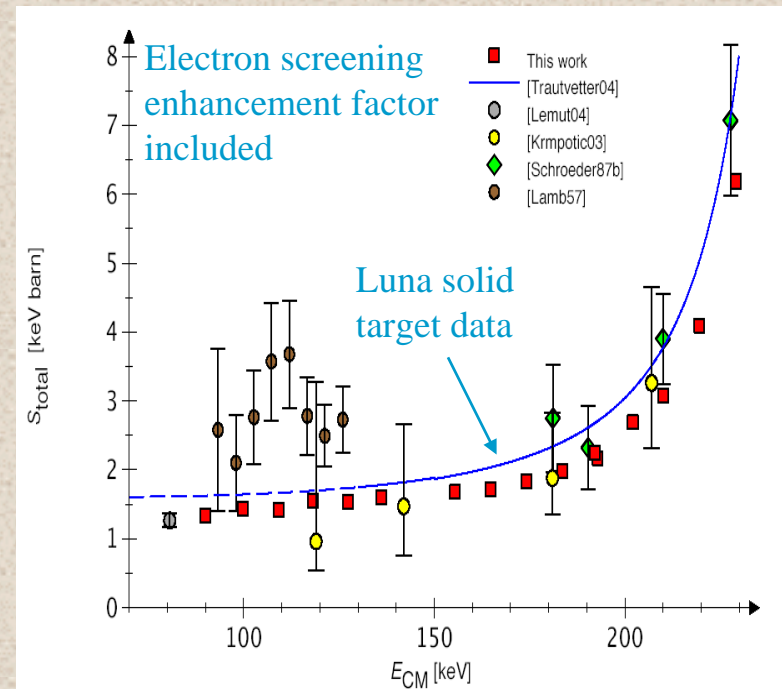
Sample BGO spectrum at $E_p=100$ keV;
Duration – 5 days; Accumulated charge- 131.6 C



SINP 18/01/2006

SLENA2006

Astrophysical S-factor from direct measurements.



- At stellar temperatures $T \leq 3 \times 10^8 \text{K}$, the reaction rate is dominated by the tail of the -507 keV resonance.
- At temperatures $T \geq 3 \times 10^8 \text{K}$, the $1/2^+$ resonance at $E_r = 0.259 \text{ MeV}$ dominates the reaction rate. Interference effects between several $3/2^+$ higher energy lying resonances must also be considered.

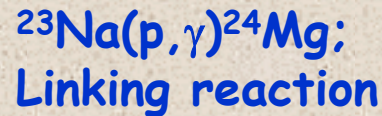
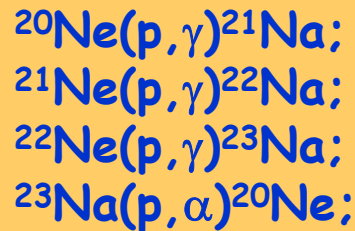
How can FRENA contribute?

- Existing data reported in the energy region 400-600 keV show wide discrepancies.
- Hence, the need to study the reaction at higher proton energies in a single experiment.

Other important reactions of the CNO cycle

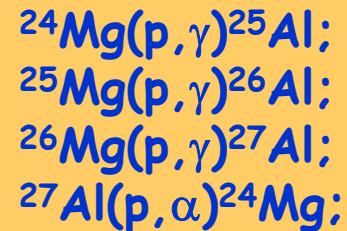
- The hydrogen burning of ^{19}F via the competing reactions $^{19}\text{F}(p,\gamma)^{20}\text{Ne}$ and $^{19}\text{F}(p,\alpha)^{16}\text{O}$ decide if the CNO cycle ceases and the NeNa cycle is initiated.
- Further studies of these two reactions at low energies, preferably below 250 keV are required.

Reactions of the NeNa cycle



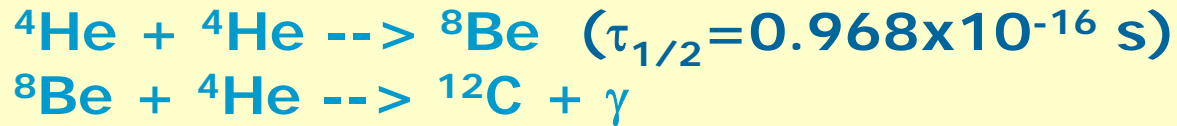
The reaction rates for most of these reactions are well studied over certain stellar temperature ranges only. These reactions should be studied over a wider range of energies for the proton beam.

Reactions of the MgAl cycle



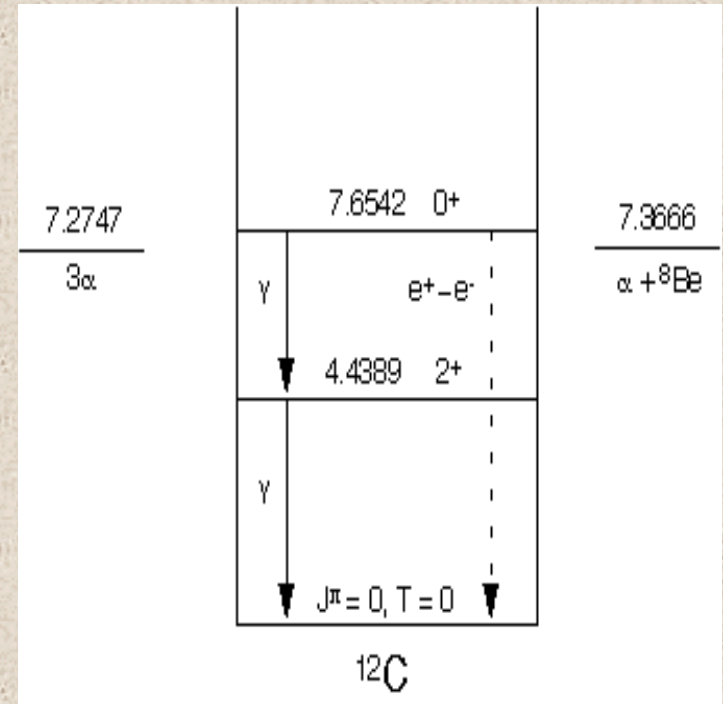
The reaction $^{27}\text{Al}(p,\alpha)^{24}\text{Mg}$ provides the return path to the MgAl cycle. Hence, this reaction is important. Should be studied down to energies below 500 keV where resonances are expected.

Helium Burning



The triple α reaction leaps from helium to carbon in one go, bypassing Li, Be and B. It is no coincidence that these 3 elements are over 10^5 times less abundant than carbon.

The ${}^{12}\text{C}$ is formed fortuitously in the triple alpha reaction due to the presence of the 7.6542 MeV resonance state.

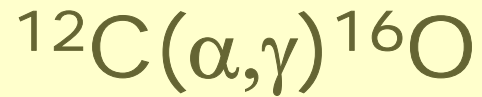


alpha + ^{12}C capture

Probably the most important reaction in Nuclear Astrophysics now

- Its rate relative to the 'triple- α ' capture determines what fraction of ^{12}C is converted to ^{16}O ; i.e. C/O ratio in red giants.
- The C/O ratio at the end of He-burning phase sets the initial condition for the heavy-ion burning.
- Depending on the stellar mass, the HI burning leads to several possibilities that include white dwarfs and supernova.

$\langle\sigma v\rangle$ depends on $S(E)$ at the Gamow energy $E_0=0.3$ MeV for He-burning temperatures; i.e. $T_9=0.2$.



E_{cm} (MeV)	θ_{max} (°)	S_{E2}/S_{total}	S_{total} (keV·b)	σ (pb)	Rate ($100\text{p}\mu\text{A}\cdot 10^{18}\text{cm}^{-2}$) (fusions/day)
2.4	1.2	0.038	68	49000	3×10^6
2.0	1.2	0.1	31	7500	4×10^5
1.4	1.4	0.25	29	590	3×10^4
1.0	1.6	0.34	31	36	2000
0.8	1.7	0.36	34	4	200
0.7	1.8	0.38	40	1	50
0.6	1.9	0.40	50	0.3	16
0.5	2.1	0.60	60	0.03	2

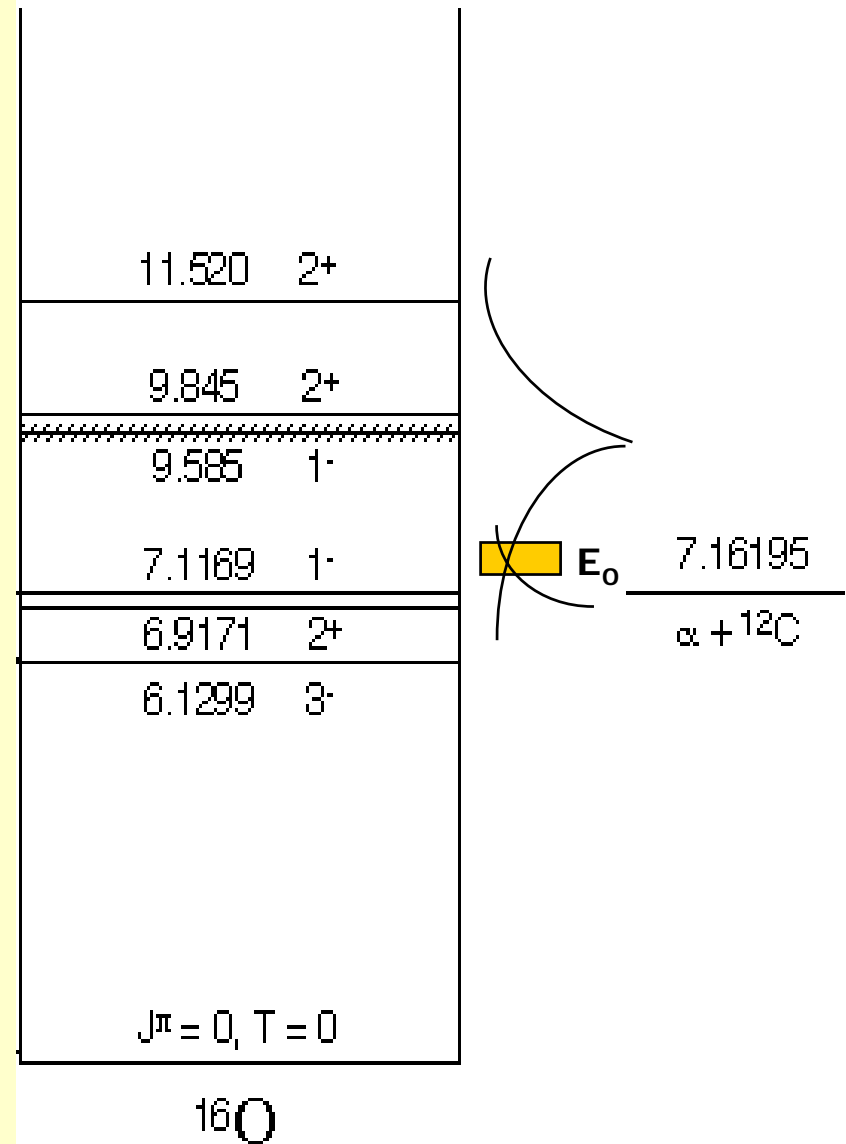
J.M.L. Ouelett et al., Phys. Rev. C 54(1996)1982.

- Efforts are being made to make measurement at or near E_0 and also from inverse reactions.
- The cross-sections at astrophysical energies is dominated by the $E1$ and $E2$ capture to ^{16}O ground state.
- Extrapolation to low energies is guided by reaction theories that use different approaches such as R-matrix, K-matrix.
- Apart from $^{12}\text{C}(\alpha,\gamma)^{16}\text{O}$ data, additional data such as
 - ^{16}O bound state properties,
 - $^{12}\text{C}(\alpha,\alpha)$ scattering,
 - β -delayed α -particle spectrum from ^{16}N and
 - α -transfer reactions on ^{12}C

are incorporated using R- and K-matrix theories to constrain the extrapolation.

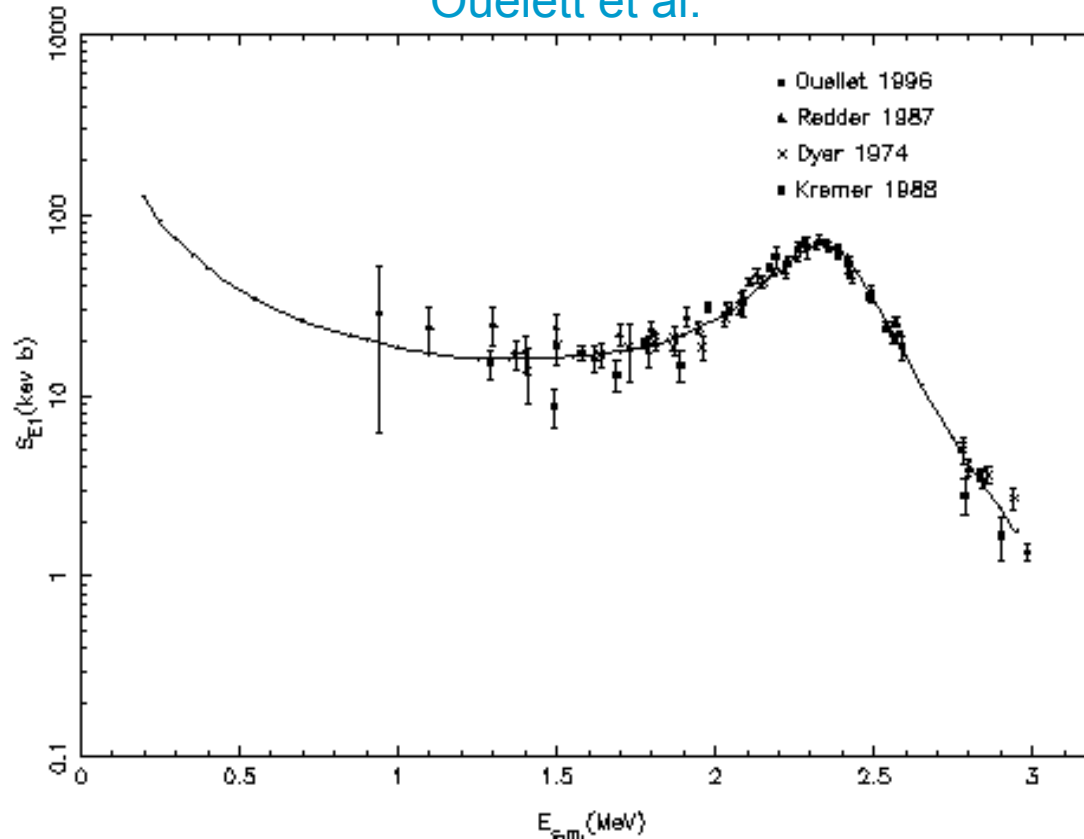
● $S_{\text{cap}}(E) = S_{E1}(E) + S_{E2}(E).$

● The $E1$ and $E2$ components are extrapolated separately to E_0 due to their different energy dependence, both being influenced by the presence of sub-threshold bound states in ^{16}O having $J^\pi = 1^-$ (-45 keV) and 2^+ (-245 keV), respectively.



Extrapolated values of $S_{E1}(E_0=0.3 \text{ MeV})$ obtained from direct measurements of the differential capture cross section.

Reference S-factor plot for $\alpha+^{12}\text{C}$ E1 capture from the R-matrix fit of elements
Ouellet et al.



Dyer, P. and
Barnes, Nucl
A233(1974)

A. Redder et al.
Phys. A462(1987)

R.M. Kremer et al.
Phys. Rev. Lett.
60(1988)147

J.M.L. Ouellet et al.
Phys. Rev. C
54(1996)198

used for E2
capture Calc.

for E1 and

gamma
emission

for E1 and

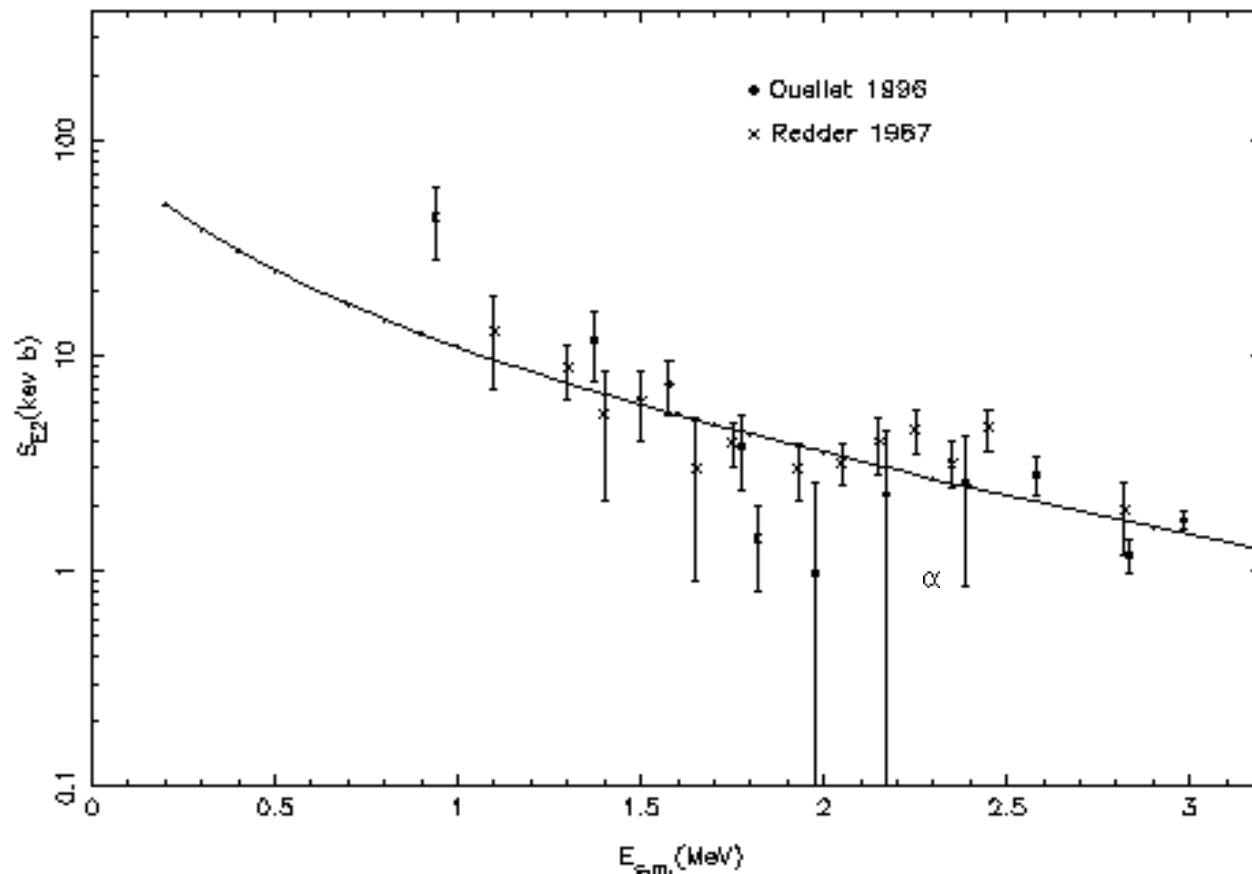
Extrapolated values of $S_{E2}(E_0=0.3 \text{ MeV})$ obtained from direct measurements of the differential capture cross section

A. R.
Phys

H.P.
Proc
the C
Phys

J.M.
Phys
54(1)

S-factor plot for $\alpha + {}^{12}\text{C}$ E2 capture from the *cluster model* calculation of Ouelett et al.



ements

l E1 and

l E1 and

l E1 and

Using the results of Ouelett et al.,

$$S_{\text{cap}}(E_0) = 120 \pm 40 \text{ keV-b for } {}^{12}\text{C}(\alpha, \gamma){}^{16}\text{O}$$

- These values are quite consistent with the best estimates obtained by the TRIUMF group and with many of the earlier direct measurement.
- However, it should be remembered that some of the recent data and analyses continue to indicate lower values of the E1 S -factor.
- While the uncertainties of these important parameters are gradually decreasing with time, they remain well outside of the 10-15% level that is desirable for astrophysical applications.

Clearly, more work remains to be done on $\alpha+{}^{12}\text{C}$ capture, especially concerning the extrapolation of the E2 S -factor. Experiments in the inverse kinematics will be useful. Measurements at $E_{\text{cm}} \leq 2.4 \text{ MeV}$ ($E_{\text{lab}} \leq 3.2 \text{ MeV}$) required where there are rather large discrepancies in the existing data.

Other He-burning reactions

• The reaction $^{16}\text{O}(\alpha,\gamma)^{20}\text{Ne}$ proceeds at a slow rate at $T_9 = 0.1-0.2$, because of the larger Coulomb barrier and the properties of the states near E_0 . Above, $T_9 = 0.3$, the rate exceeds that of $^{12}\text{C}(\alpha,\gamma)^{16}\text{O}$ due to resonances at high energy.

• Neutron producing reactions:

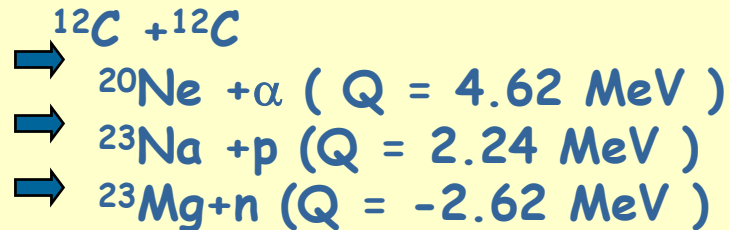
$^{13}\text{C}(\alpha,n)^{16}\text{O}$, $^{17}\text{O}(\alpha,n)^{20}\text{Ne}$, $^{18}\text{O}(\alpha,n)^{21}\text{Ne}$, $^{21}\text{Ne}(\alpha,n)^{24}\text{Mg}$,
 $^{22}\text{Ne}(\alpha,n)^{25}\text{Mg}$, $^{25}\text{Mg}(\alpha,n)^{28}\text{Si}$, $^{26}\text{Mg}(\alpha,n)^{29}\text{Si} \Rightarrow$ s-process

→ Problem - $^{14}\text{N}(n,p)^{14}\text{C}(e-n)^{14}\text{N}$ consumes the neutrons

- Although experimental data do exist, each of these reactions present a separate problem. Need to study nuclei in the s-d shell ($A \sim 24$) where states near the particle threshold are expected.
- Need to study the competing (α,γ) reactions for a more precise understanding of the rate of neutron production; especially $^{22}\text{Ne}(\alpha,\gamma)^{26}\text{Mg}$ for which information are insufficient.

Heavy-ion burning

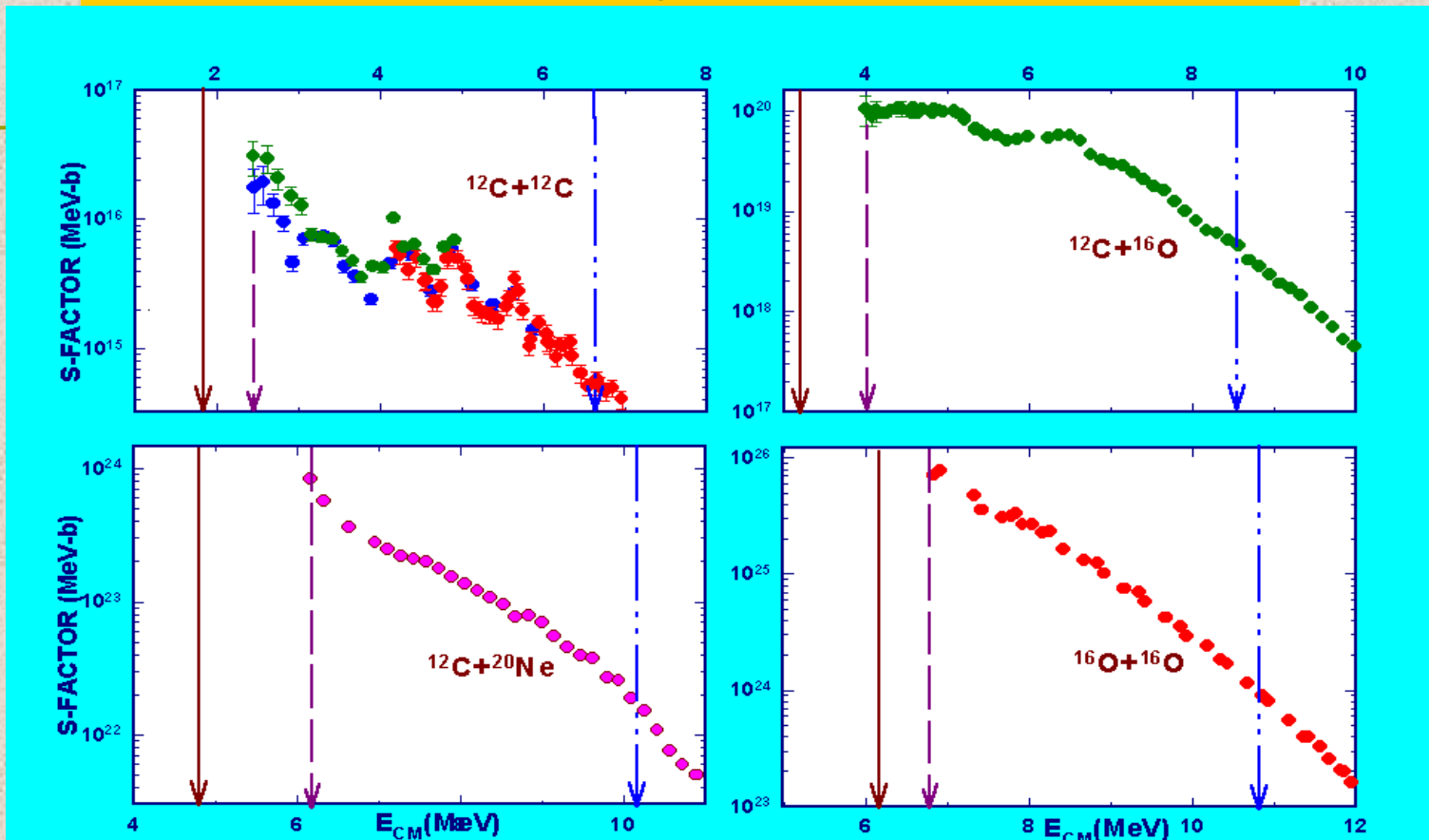
- HI burning is important in stellar evolution & nucleosynthesis
- After He-burning, gravitational contraction leads to large increase in temperature and density in the core to ignite C & O ashes.
- Since Coulomb barrier is the lowest for $^{12}\text{C} + ^{12}\text{C}$, they will react first.



- Subsequently, other HI reactions occur, dictated by their Coulomb barrier and Q-values



Plots of S-factor vs E_{cm} for the 4 HI reactions



Interesting observations

- $^{12}\text{C} + ^{12}\text{C}$ show pronounced resonance structures at sub-barrier energies
- $^{12}\text{C} + ^{20}\text{Ne}$ and $^{16}\text{O} + ^{16}\text{O}$ do not show structures
- Theoretical models do not provide a consistent explanation.

Need for Experiments

In $^{12}\text{C} + ^{12}\text{C}$ for example, data exists only up to $E_{\text{cm}} = 2.46 \text{ MeV}$

Reason

- Presence of H & D contaminant in C target whose reaction with ^{12}C results in large Compton background masking weak γ -ray speaks.

NEW EXPERIMENTAL TECHNIQUES NEEDED

- High beam currents
- Clean targets
- Use of Compton suppressed Clover detectors

However, as cross-sections decrease by orders of magnitude for even a small decrease in incident energy, **EXTRAPOLATION TO LOWER ENERGIES IS UNAVOIDABLE.**

FOR THIS, REACTION MECHANISM MUST BE UNDERSTOOD.

- Although s-factor should be featureless for well-behaved systems, rich and puzzling structures are observed.
- Therefore, apart from the 4 HI reactions, study of other reactions is also important.
- Scope for studying these reactions below Coulomb barrier.

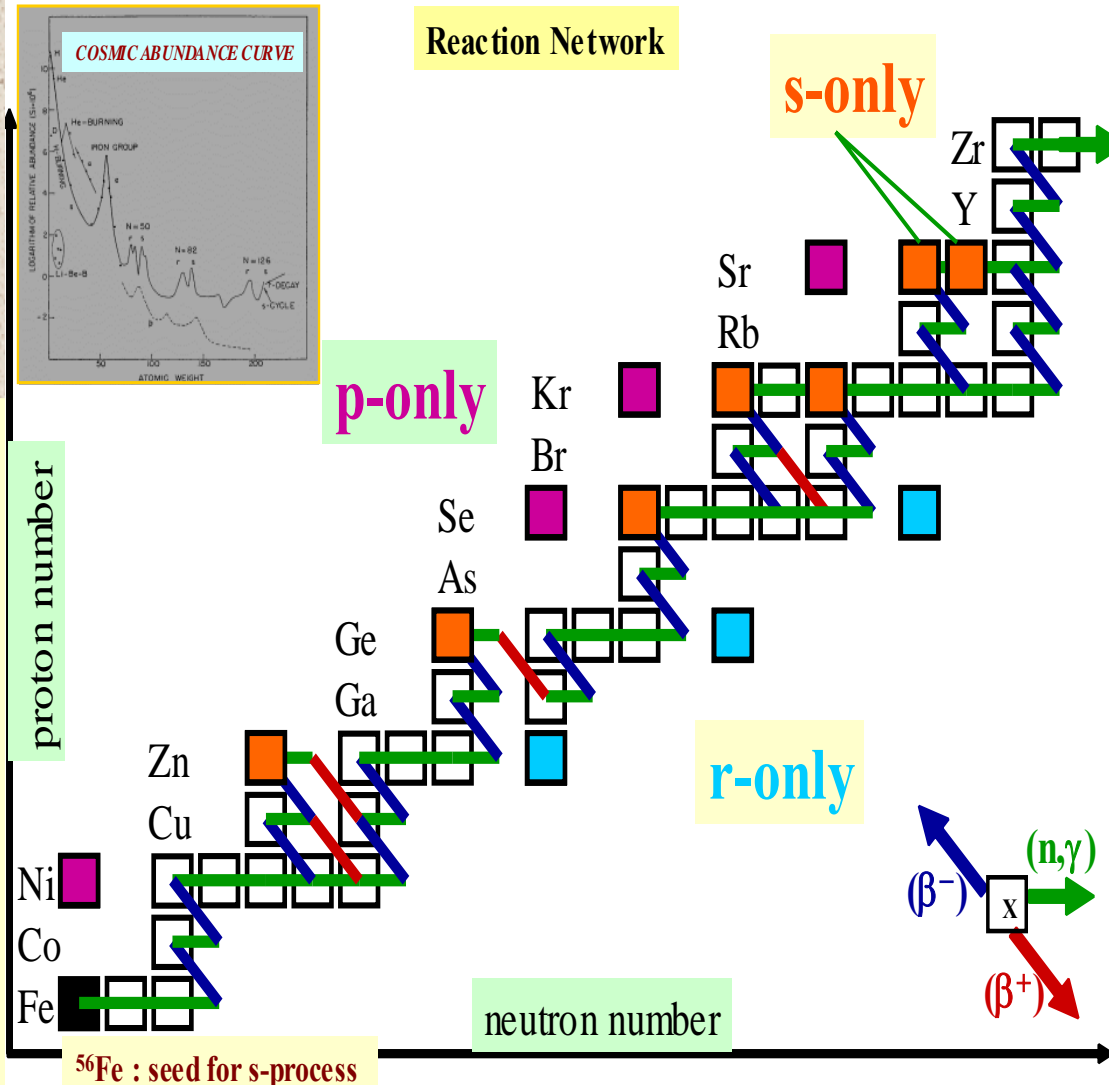
Syntheses of elements heavier than ^{56}Fe

Does not occur through fusion reactions because

- Coulomb barrier increases with Z ; σ will fall drastically.
- BE/A for ^{56}Fe is max.; hence no energy is released.

Heavy elements are synthesized through the s-, r- and the p-processes.

The general pattern of elements in our solar system => for s-process $\tau_{n\gamma} \gg \tau_{\beta}$ (β -decay lifetimes). The required neutron density is $N_n \sim 10^8$ neutron/cm³

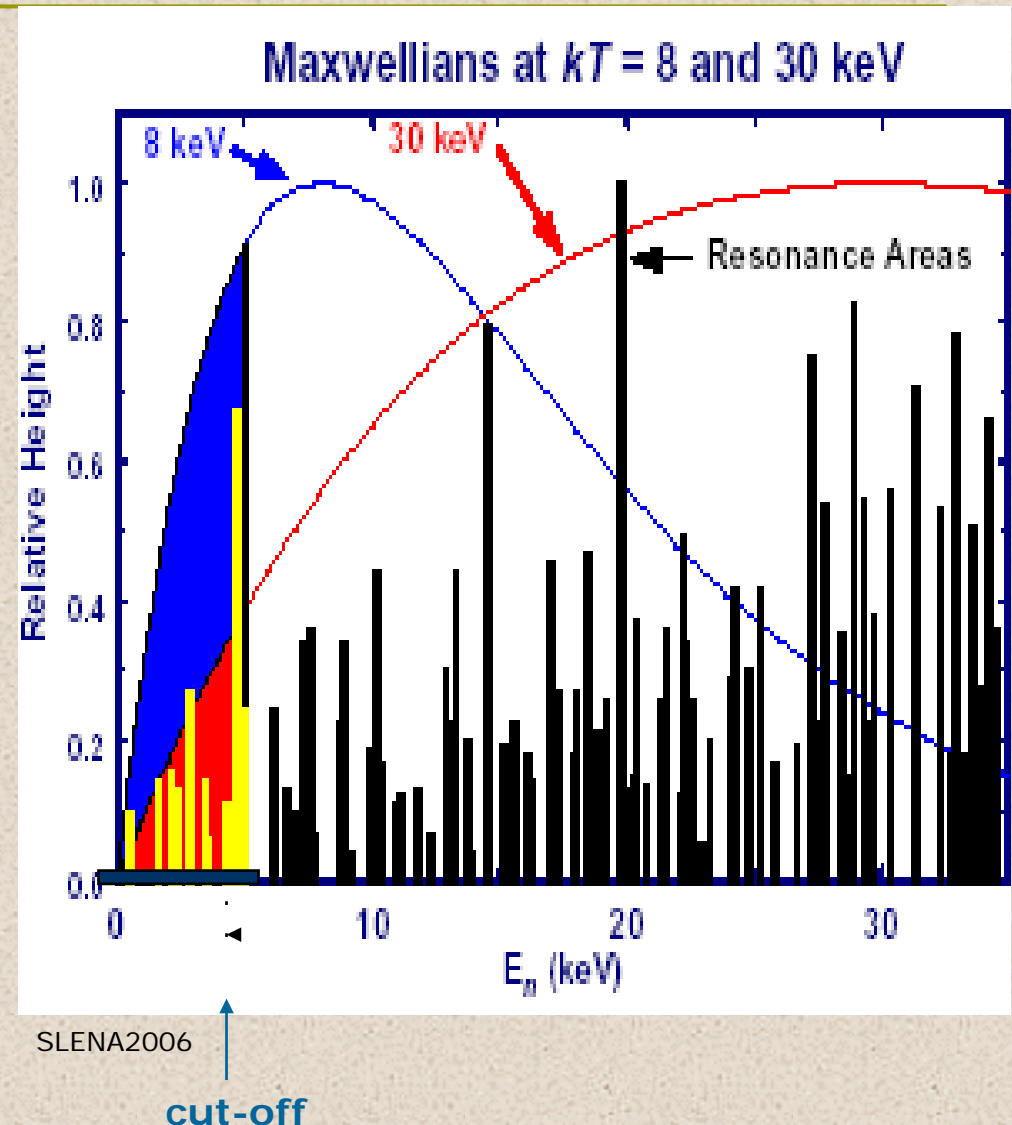


● One major difference between classical and new s-process models is the temperature at which most of the neutron exposure occurs.

- From classical s-process models, $kT=30$ keV.
- Recent calculations show that in low mass red giants, most of the neutron exposures occurs at $kT = 6-8$ keV

About 80% of new ORELA data → extrapolations are in error by 2 to 3 times the estimated uncertainties; hence, they do not test the new stellar models.

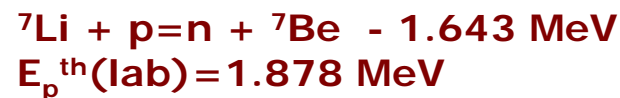
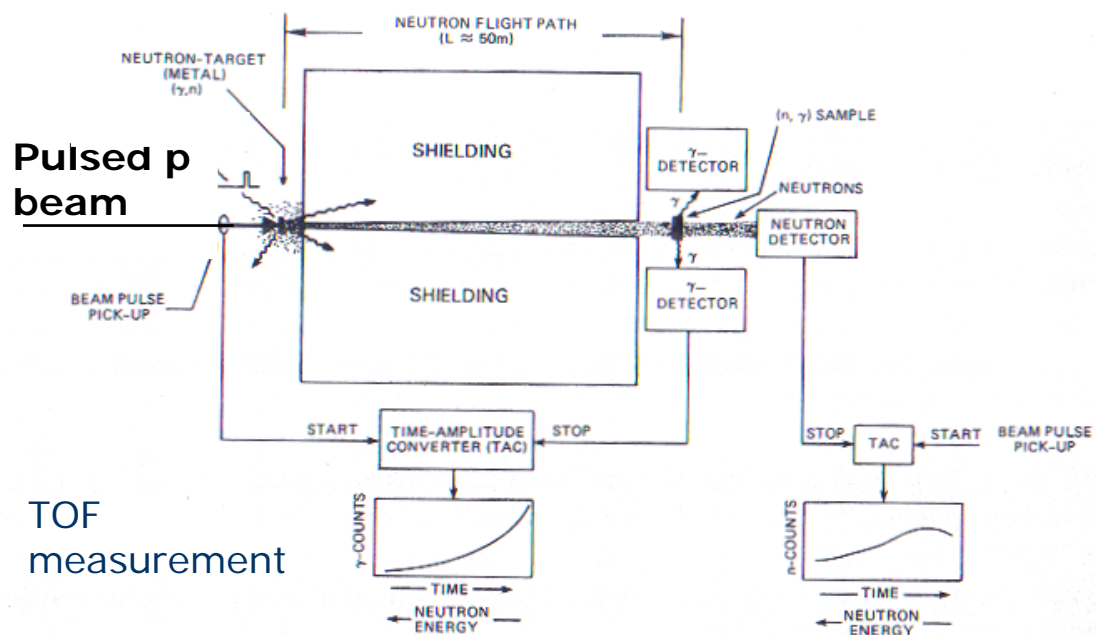
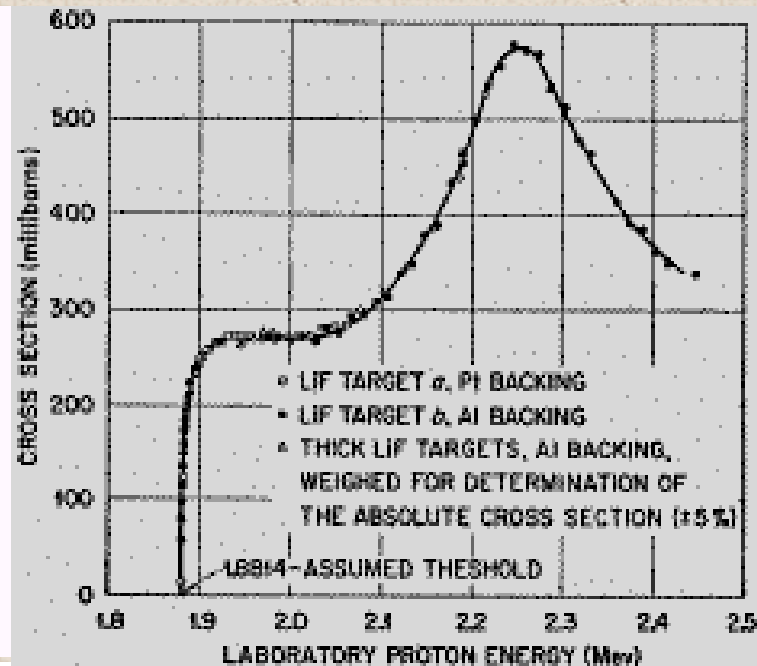
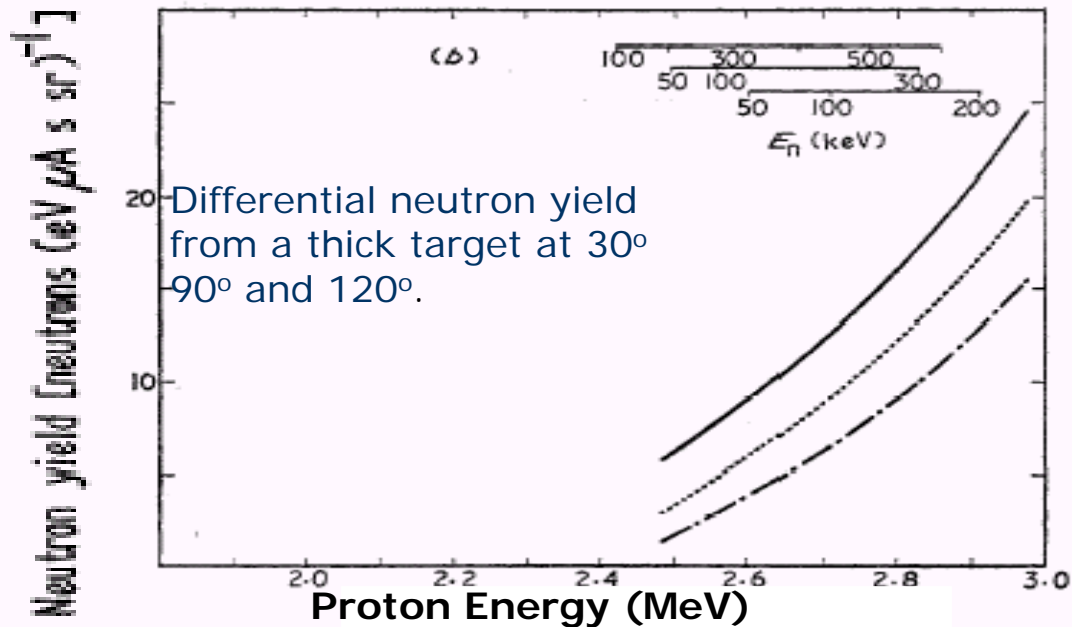
Therefore, direct meas. of cross sections to lower energies are needed.



Several outstanding questions in Nuclear Astrophysics that require new experiments:

- The s-only isotopes are the most important calibration points for models. New precise (n, γ) measurements at low neutron energies are required to determine the reaction rates for these isotopes near $kT=6-8$ keV so as to test the new stellar models.
- Observational data on the composition of meteorites, which are believed to have been formed in red giants where s-process had occurred, have led to stellar and galactic chemical evolution models. Very few (n, γ) rates are known to test these models.
- The r-process abundances (the main constraint on r-process models) are derived from the measured solar abundances by subtracting the calculated s-process contributions. Therefore, a reliable model for the s process is important for a better understanding of the r-process. It is therefore important to make new (n, γ) measurements.

- Clearly, there is ample scope for carrying out new n-capture measurements, especially at low energies.
- Using suitable reactions, like ${}^7\text{Li}(p,n){}^7\text{Be}$ [$E_{\text{th}}(\text{Lab.})=1.878 \text{ MeV}$] with high current pulsed beams from the proposed 3 MV accelerator, good quality pulsed neutron beams can be produced.
- The time-of-flight technique (TOF) based on the detection of the prompt capture gamma rays can be used to do new n-capture cross sections measurement.
- The activation method, can also be applied to these measurement



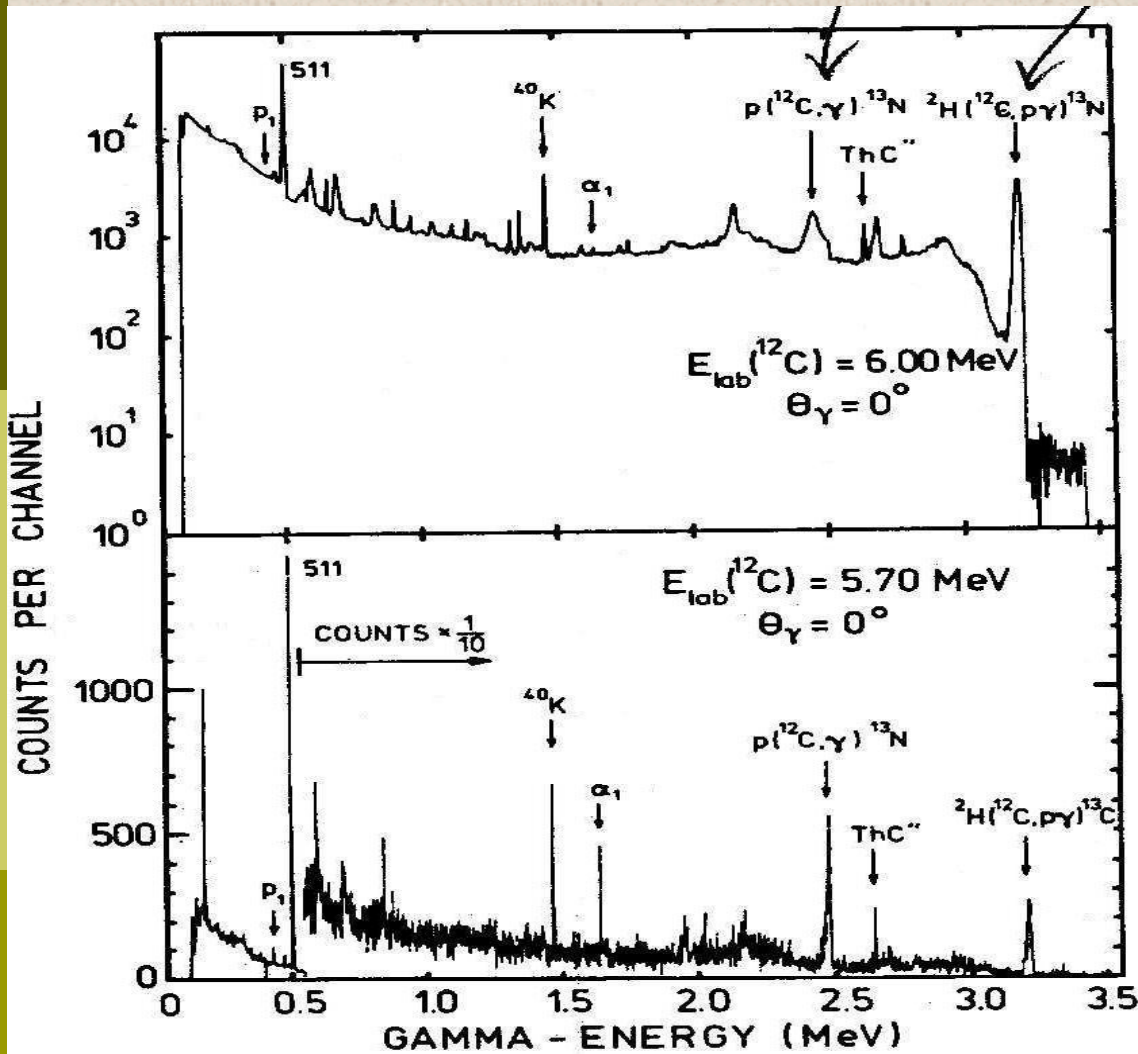
${}^7\text{Li}(p,n){}^7\text{Be}$ reaction cross section as a function of incident proton energy

Problems associated with the measurement at low energies

1. Background

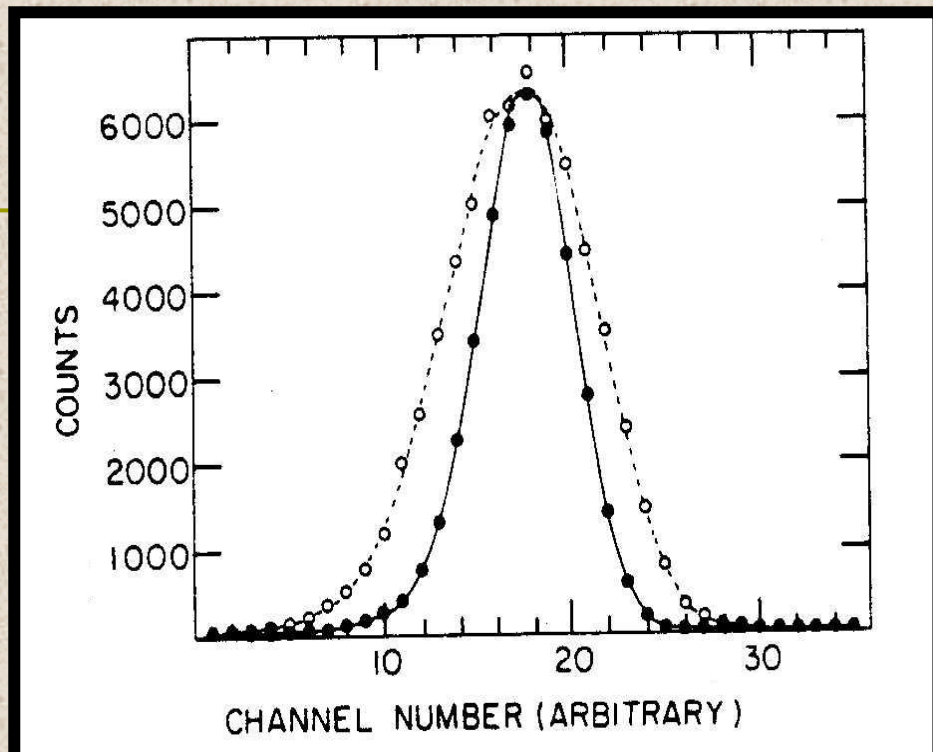
- a) Room background [^{40}K , Ra-series, Th-series]
- b) Beam background
- c) Background arising from the reactions with impurities in the target.

The seriousness of the background is best illustrated with an actual measurement e.g. $^{12}\text{C}+^{12}\text{C}$ reaction at $E_{\text{cm}}=5.70$ and 6.0 MeV.



The γ -ray spectrum (a) is dominated by background from the interaction of ^{12}C beam with the ^1H and ^2H contaminations (few atoms %) in the target. Spectrum (b) is obtained with a $13 \mu\text{g}/\text{cm}^2$ target having low hydrogen contamination (0.2 atoms %). The well-known $E_p = 457 \text{ keV}$ resonance ($\Gamma = 39 \text{ keV}$) in $^{12}\text{C}(p,\gamma)^{13}\text{N}$ corresponds in the inverse reaction $^1\text{H}(^{12}\text{C},\gamma)^{13}\text{N}$ corresponds to an energy of $E_{\text{cm}}(^{12}\text{C} + ^1\text{H}) = 2.74 \text{ MeV}$.

$p_1 \Rightarrow 0.440 \text{ MeV}$ γ -ray of ^{23}Na in the $^{23}\text{Na}+p$ channel.
 $\alpha_1 \Rightarrow 1.634 \text{ MeV}$ γ -ray of ^{20}Ne in the $^{20}\text{Ne}+\alpha$ channel



the shapes of the elastically scattered peaks at the beginning (●) and at the end (○) of the experiment. The lines joining the points are the Gaussian (asymmetric) fits to the data giving standard deviations $\sigma = 2.4$ channels and $\sigma = 4.2$ channels, respectively.

2. Carbon deposition in the target

It is a serious problem when the targets are thin.

This is illustrated with $^{12}\text{C}+^{12}\text{C}$ reaction where the elastically scattered events were detected with a S.B. detector.

3. Effective energy

For thin targets and high incident energy,

$$E_{\text{eff}} = E_0 - \Delta E / 2$$

For relatively thicker targets and low incident energy the integrated cross-section is measured from

$$E_0 - \Delta E \text{ to } E_0.$$

In this case an effective energy E^* is defined so that,

$$\sigma(E^*)\Delta E = \int_{E_0 - \Delta E}^{E_0} \sigma(E) dE$$

For a $100\mu\text{g}/\text{cm}^2$ target of ^{12}C in the $^{16}\text{O} + ^{12}\text{C}$ reaction at $E_{\text{cm}} = 4.0 \text{ MeV}$, E^* is found to be 50 keV more than that obtained using $E_{\text{eff}} = E_0 - \Delta E / 2$.

The above fact limits the use of greater target thickness to obtain greater yield.

Possible improvements in the measurement

i) *Reduction of background:*

Background due to hydrogen in the target.

Investigation by Kettner et al. [Z. Phys. A298(80)65]

a) Maximum hydrogen concentration at the top and bottom layers of a carbon target.

b) Baked Ta does not contain hydrogen.

Hydrogen in the bottom layer could be removed using carbon deposition on to a baked Ta foil. More research is required to have hydrogen free targets.

ii) *Reduction of Compton background*

At lower energies ($E_{\text{cm}} < 2.46 \text{ MeV}$) Compton background from 2.36 MeV γ -ray completely masks the ^{20}Ne and ^{23}Na γ -lines.

Reduction of Compton background can be made using

- i) Compton suppressed HPGe detectors
- ii) Compton suppressed clover detectors
- iii) Array of such detectors.

iii) Use of large *beam current*

$$N_{\gamma} = (\sigma \epsilon N_T) N_B$$

As N_T cannot be increased, to increase N_{γ} , N_B has to be increased. One must have an accelerator delivering high current.

Also, proper cooling is essential for the targets.
Thin target with Ta-backing

**THANK
YOU**